Sven-Thomas Antoni*, Stefan Soltau, Jens Beringhoff, Omer Rajput, Christoph Otte, and Alexander Schlaefer

Enhancing haptic feedback of subsurfaces during needle insertion

https://doi.org/10.1515/cdbme-2018-0150

Abstract: Haptic feedback can be helpful for accurate needle insertion but is complicated by friction on the needle shaft. Concepts to directly measure the forces at the needle tip exist but cause additional cost and complexity. Moreover, haptic devices may show inaccuracies in recreating forces.

We present a novel force feedback method that uses needle shaft forces and enhances haptic feedback of subsurfaces based on robotic ultrasound elastography. This approach allows to overcome accuracy limitations of haptic devices.

We evaluate our method in a volunteer subject study using recordings from a robotic needle driver setup. We compare haptic feedback based on shaft and enhanced force for the detection of surfaces inside of gelatin phantoms. Using our method, the error of subsurface detection decreased from more than 16 to about 1.7 mm for the first subsurface. A second subsurface was solely detectable using our method with an error of only 1.4 mm. Insertion time decreased by more than 32%.

The results indicate that our enhanced sensor is suitable to detect subsurfaces for untrained subjects using a haptic feedback device of limited accuracy.

Keywords: Haptic feedback; needle insertion; elastography

1 Introduction

Haptic sensation is often the only available tissue information during needle insertions, e.g., for biopsies or brachytherapy. For correct needle placement, detecting subsurface structures is important but increasing friction forces make it difficult to sense changes in the mechanical properties of deeper tissue. [1].

Robotic needle driving has been studied for various applications [1, 2]. However, most systems are not able to insert needles fully autonomously but assist a human operator during needle placement. This assistance often includes feeding back forces as well as providing image guidance using, e.g., ultrasound (US) or magnetic resonance imaging (MRI) [2].

Haptic feedback can be realized by using force measurements from conventional force-torque sensors at the needle shaft. However, the shaft force is superimposed by large frictional forces. To overcome this issue, the needle tip forces could be measured and fed back [1]. Several sensors have been proposed to directly measure needle tip forces, i.e., mechatronic sensors [3, 4] and fiber optical force sensors [5–7]. It has been shown that subsurface detection can be improved by feeding back needle tip forces instead of shaft forces [1]. Unfortunately, adding a tip force sensor would require additional costs and effort.

Usually, it is not possible to identify changes in the elastic tissue behavior with the help of MRI or US. Instead, elastographic imaging can be used to determine elastic tissue properties. US's high inter-operator variability [8] has led to the development of different robotic US systems [8, 9].

We propose an enhanced force sensor using robotic US elastography (USE) to amplify subsurface structures in the shaft force signal. The force can be provided to a physician as hapic feedback. We show that force reproduction of haptic feedback devices can lead to errors in the range of forces present during surface penetration. Solving this issue solely by scaling the forces would quickly result in too high forces. Hence, we demonstrate that a moderate scaling combined with our USE based enhancement is suited for subsurface detection.

We evaluate our setup with volunteer subjects and compare the detection of subsurface structures for haptic feedback based on the needle shaft force and our enhanced feedback force. We describe our calibrated and synchronized robotic needle driving and robotic USE setup used to record the data. Moreover, we present results indicating that by using our method, subsurface structures inside gelatin can be precisely identified by untrained subjects for different friction forces.

2 Materials and Methods

2.1 Recording Setup

Our data recording setup includes two robotic devices. We use a PI H-820 hexapod (Physik Instrumente, Germany) to articulate the needle. Additionally, a UR3 robot (Universal Robots, Denmark) with a L14-5/38 linear US probe attached to

***Corresponding author: Sven-Thomas Antoni, Stefan Soltau, Jens Beringhoff, Omer Rajput, Christoph Otte, Alexander Schlaefer,** Institute of Medical Technology, Hamburg University of Technology, Germany, e-mail: antoni@tuhh.de - S.-T. Antoni and S. Soltau contributed equally

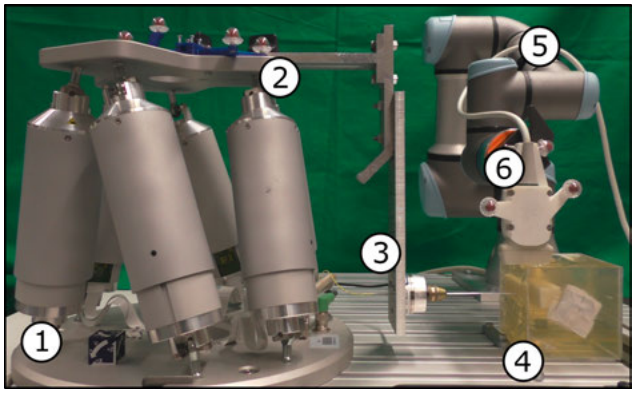

Fig. 1: Data recording setup with hexapod (1), camera markers (2), force torque sensor with attached needle (3), gelatin phantom with embedded structure (4), UR3 robot (5) and US probe with camera markers (6). Not depicted are the US device, the baseplate marker geometry and the tracking camera.

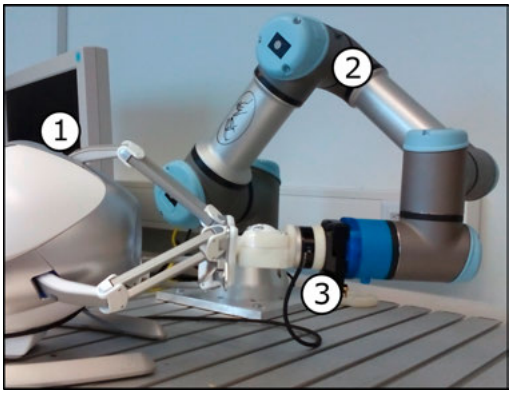

Fig. 2: Novint Falcon (1) calibration setup with UR3 robot (2) and FT sensor (3)

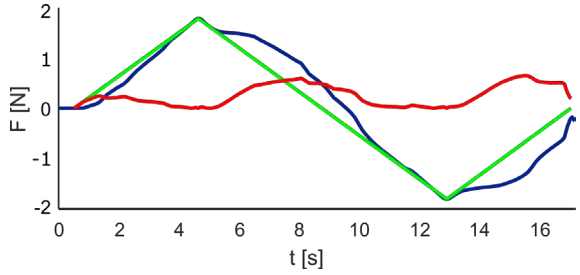

Fig. 3: Feedback forces of a calibrated Falcon: commanded (green) and measured (blue) feedback force as well as force error (red)

a SonixTOUCH US (Analogic Corporation, MA, US) is used for imaging. See Fig. 1 for an overview of the recording setup.

In order to perform strain USE, the tissue is repeatedly compressed with the probe by the UR3. Additionally, when the needle tip moves closer to the border of the US image, the probe is moved by the UR3 to follow the needle trajectory.

Using attached marker geometries and a fusionTrack 500 (Atracsys, Switzerland) tracking camera, the setup is thoroughly calibrated. The US is calibrated by using a 3D-printed Z-Phantom [10], whose wire placement was validated by using the tracking system. Utilizing the tracking camera, both robots are calibrated with respect to the baseplate by hand-eye calibration using the QR24 algorithm [11].

2.2 Recorded data

For data recording, we insert the needle into three different gelatin phantoms, which are placed in acrylic glass boxes. To simulate subsurfaces, a block of dense gelatin ($30 \times 30 \times 80$ mm^3) is embedded in soft gelatin. The Young's moduli are about 22 and 90 kPa for soft and dense gelatin, respectively. Overall, 18 needle insertions are recorded.

During insertion, the USE images and the needle shaft forces are recorded synchronously at 16 and 500 Hz, respectively. The gray values of USE and the shaft forces are filtered with a running median width 10 and 1000, respectively. Through synchronizing the devices to a local time server, we can represent the recorded data in a single time domain.

Different friction forces are simulated by inserting the needle at a constant speed of 1 mm/s through foam (26 kg/m^3) of different thickness (11, 13.3 and 26.6 mm) that is placed in front of the gelatin phantom.

2.3 Haptic Feedback Generation

For our trial, we use a Falcon haptic feedback device (Novint Technologies, NM, US) with the standard ball grip. The Falcon is a consumer grade 3-DOF system and its feedback forces are displayed relatively inaccurately [12]. We use a calibration setup to evaluate the accuracy and repeatability of the Falcon device with a conventional force-torque sensor. For this purpose, the grip of the Falcon is fixated at different positions of its workspace with the help of the UR3 robot. See Fig. 2 for an overview of the setup. At each position, forces of 3 N are applied and measured in the positive and negative direction of all three axes. Preliminary experiments showed a mean error on the calibration data of 1.02 ± 0.39 N before and 0.08 ± 0.2 N after calibration. On an independent validation set the error was 0.24 ± 0.17 N.

In our data, forces of up to 2 N and rates of change of no more than 0.1 N/s occur at the needle shaft. Hence, feeding back the actual needle shaft forces seems infeasible. Additionally, the feedback force error of the Falcon does not behave linearly, see Fig 3.

To overcome the limitations of the haptic feedback device, we developed a novel method for enhanced generation of feedback forces based on USE. First, we evaluate the tissue stiff-

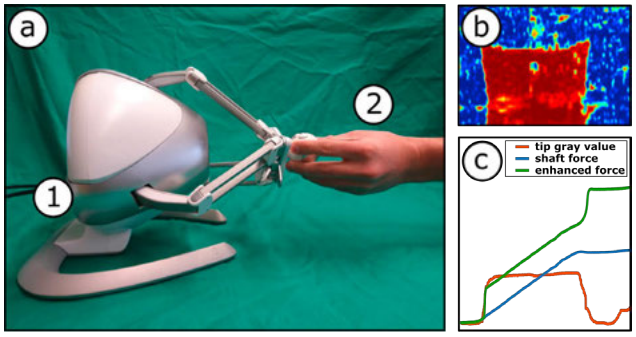

Fig. 4: Trial setup (a) with haptic feedback device (1) and subject (2). The recorded USE image is depicted in (b). The haptic feedback of shaft (blue) and enhanced (green) force are plotted in (c) alongside the USE gray value along the needle trajectory (red).

ness (expressed as gray value) directly in front of the needle tip using the USE image data, compare Fig. 4b,c. We then add an offset of 1 N to the shaft force each time the gray values exceed and fall below 128. This change is assumed to correspond to subsurfaces. For our experimental setup, this corresponds to the needle's insertion and exit point.

The different force data, i.e., shaft and enhanced force, is amplified by a factor of two and fed back to the device.

2.4 Trial Data and Evaluation

For every volunteer subject, 5 random data sets of different friction were selected. For all randomly selected data sets, the subjects virtually inserted the needle using only the shaft force and the enhanced force, respectively. The subjects were supposed to press a button, when noticing a virtual subsurface. It was only allowed to insert the needle, pulling back was prevented by the device. See Fig. 4a for an overview of the setup.

Afterwards, we calculated the absolute distance between each detected and actual subsurface position.

3 Results

In total, 13 subjects took part in our trial. Hence, 65 runs were performed with shaft forces and enhanced forces, respectively. None of the subjects detected the exit point using shaft forces only, see Table 1 for an overview of our results.

4 Discussion

In general, all subjects were able to determine subsurfaces more accurately with our enhanced force sensor. On average, 8 and 9 subjects had a detection error smaller than 2 mm for the insertion and the exit, respectively. In general, most subjects had no problems operating the haptic feedback device, compare Table 1. Subject 4 had noticeable problems but still performed better with the enhanced forces than only shaft forces and subject 10 failed to detect the exit using the enhanced forces. Even including subject 4, the mean error of detecting the insertion point using the enhanced forces was only about 14% of the error when using the shaft forces. Subject 4 excluded, the average error for detecting the exit and insertion point for enhanced feedback is 1.7 and 1.4 mm, respectively. This is even more impressive compared to the more than 16 mm error of the shaft force based detection; especially taking into account that the high density gelatin block is only 30 mm in diameter.

Remarkably, no subject was able to detect the exit point using solely shaft forces and a later dialog with the subjects revealed that they were guessing the insertion positions rather than really feeling them. Clearly, the shaft forces are not feasible for subsurface detection. Even scaling the shaft forces did not improve this. While at higher scaling the subsurface may become noticeable, the maximum forces would quickly exceed the exertion force of the haptic feedback device. A scaling factor of 4 would suffice to exceed 8.9N, the maximum exertion force of our device, while only giving a maximum of 0.4 N/s to sense which is still smaller than the observable force errors.

Not only did the force feedback based on the enhanced sensor yield a more precise subsurface detection, it also allowed for much faster insertions. On average, subjects performed more than 32 % faster using the enhanced forces compared to using shaft forces only, compare Table 1. Many subjects were able to halve the insertion time while still improving their results very noticeably. Moreover, the standard deviation of the error is more than 70 % smaller for the enhanced sensor. Both results can be traced back to the fact that the shallow gradient of the shaft only feedback force does not allow for distinct estimation of the tissue properties at the needle tip.

5 Conclusion

Overall, the enhanced forces are able to reduce subsurface detection errors by more than 900% on average and insertion times by more than 32%. Additionally, scaling the enhanced forces is very straightforward while scaling the shaft forces does not improve detection. With US readily available during most robotized needle insertions, improving force feedback using our method seams feasible for many applications.

Tab. 1: Average insertion and exit errors in mm for the different subjects as well as the mean average errors with and without subject 4. Additionally, the average runtimes are presented. Note that no subject successfully detected the exit using the shaft forces

Subj.	insertion		exit	time	
	shaft	enhanced	enhanced	shaft	enhanced
1	9.81 ± 13.20	1.06 ± 1.65	0.49 ± 0.22	16.70 ± 2.00	12.85 ± 0.97
2	13.26 ± 5.80	2.38 ± 1.56	1.13 ± 1.72	34.84 ± 8.63	16.38 ± 2.70
3	16.23 ± 3.54	1.39 ± 0.87	0.14 ± 0.07	32.05 ± 6.78	17.98 ± 16.55
4	26.12 ± 3.70	10.66 ± 4.24	3.98 ± 2.98	21.17 ± 11.45	15.92 ± 2.68
5	18.87 ± 12.75	0.36 ± 0.34	1.63 ± 0.85	31.25 ± 22.63	13.57 ± 0.58
6	23.44 ± 7.83	1.21 ± 1.14	1.87 ± 2.39	14.12 ± 13.81	18.15 ± 3.96
7	17.86 ± 8.20	0.56 ± 0.22	0.04 ± 0.06	20.22 ± 2.57	20.89 ± 9.74
8	18.78 ± 8.60	1.77 ± 0.70	1.23 ± 1.02	15.76 ± 12.11	7.44 ± 4.41
9	13.29 ± 4.62	0.60 ± 0.56	3.53 ± 3.15	15.26 ± 3.22	10.31 ± 2.03
10	12.24 ± 5.32	2.64 ± 3.84		31.57 ± 11.44	28.54 ± 21.64
11	17.74 ± 4.40	2.68 ± 4.53	0.26 ± 0.27	22.00 ± 7.29	12.34 ± 1.22
12	11.23 ± 4.45	3.89 ± 7.11	0.68 ± 1.37	37.12 ± 18.74	18.85 ± 2.17
13	20.74 ± 11.94	1.93 ± 0.94	4.78 ± 4.85	10.02 ± 2.35	11.87 ± 3.82
mean	16.96 ± 7.76	2.41 ± 3.76	1.54 ± 2.23	23.24 ± 9.01	15.78 ± 5.40
w/o outlier	16.07 ± 7.48	1.70 ± 2.77	1.39 ± 2.13	23.41 ± 9.39	15.77 ± 5.64

Author Statement

Research funding: The authors state no funding involved.
Conflict of interest: Authors state no conflict of interest.
Informed consent: Informed consent is not applicable.
Ethical approval: The conducted research is not related to either human or animals use.

References

[1] D. de Lorenzo, Y. Koseki, E. de Momi, K. Chinzei, and A. M. Okamura, "Coaxial needle insertion assistant with enhanced force feedback," *IEEE transactions on bio-medical engineering*, vol. 60, no. 2, pp. 379–389, 2013.

[2] T. K. Podder, L. Beaulieu, B. Caldwell, R. A. Cormack, J. B. Crass, A. P. Dicker, A. Fenster, G. Fichtinger, M. A. Meltsner, M. A. Moerland, R. Nath, M. J. Rivard, T. Salcudean, D. Y. Song, B. R. Thomadsen, and Y. Yu, "AAPM and GEC–ESTRO guidelines for image–guided robotic brachytherapy: Report of Task Group 192," *Medical physics*, vol. 41, no. 10, 2014.

[3] S. P. Rodrigues, T. Horeman, P. Sam, J. Dankelman, J. J. van den Dobbelsteen, and F.-W. Jansen, "Influence of visual force feedback on tissue handling in minimally invasive surgery," *The British journal of surgery*, vol. 101, no. 13, pp. 1766–1773, 2014.

[4] C. Hatzfeld, S. Wismath, M. Hessinger, R. Werthschützky, A. Schlaefer, and M. Kupnik, "A Miniaturized Force Sensor for Needle Tip Force Measurements," *Biomedical Engineering / Biomedizinische Technik*, vol. 62, no. s1, 2017.

[5] S. Beekmans, T. Lembrechts, J. van den Dobbelsteen, and D. van Gerwen, "Fiber-Optic Fabry-Pérot Interferometers for Axial Force Sensing on the Tip of a Needle," *Sensors*, vol. 17, no. 1, p. 38, 2016.

[6] S. Kumar, V. Shrikanth, B. Amrutur, S. Asokan, and M. S. Bobji, "Detecting stages of needle penetration into tissues through force estimation at needle tip using fiber Bragg grating sensors," *Journal of biomedical optics*, vol. 21, no. 12, p. 127009, 2016.

[7] K. M. Kennedy, L. Chin, R. A. McLaughlin, B. Latham, C. M. Saunders, D. D. Sampson, and B. F. Kennedy, "Quantitative micro-elastography: Imaging of tissue elasticity using compression optical coherence elastography," *Scientific reports*, vol. 5, p. 15538, 2015.

[8] R. Kojcev, A. Khakzar, B. Fuerst, O. Zettinig, C. Fahkry, R. DeJong, J. Richmon, R. Taylor, E. Sinibaldi, and N. Navab, "On the reproducibility of expert-operated and robotic ultrasound acquisitions," *International journal of computer assisted radiology and surgery*, vol. 12, no. 6, pp. 1003–1011, 2017.

[9] S. Gerlach, I. Kuhlemann, P. Jauer, R. Bruder, F. Ernst, C. Fürweger, and A. Schlaefer, "Robotic ultrasound-guided SBRT of the prostate: Feasibility with respect to plan quality," *International journal of computer assisted radiology and surgery*, vol. 12, no. 1, pp. 149–159, 2017.

[10] P.-W. Hsu, R. W. Prager, A. H. Gee, and G. M. Treece, "Free-hand 3D Ultrasound Calibration: A Review," in *Advanced Imaging in Biology and Medicine*, C. W. Sensen and B. Hallgrímsson, Eds. Berlin, Heidelberg: Springer Berlin Heidelberg, 2009, pp. 47–84.

[11] F. Ernst, L. Richter, L. Matthäus, V. Martens, R. Bruder, A. Schlaefer, and A. Schweikard, "Non-orthogonal tool/flange and robot/world calibration," *The international journal of medical robotics + computer assisted surgery : MRCAS*, vol. 8, no. 4, pp. 407–420, 2012.

[12] H. Qin, A. Song, Y. Liu, G. Jiang, and B. Zhou, "Design and Calibration of a New 6 DOF Haptic Device," *Sensors (Basel, Switzerland)*, vol. 15, no. 12, pp. 31 293–31 313, 2015.